Schlumberger

Cased Hole
DSI* Sonic Processing
Report

Products:	• MPS: Compressional Slowness • UDP: Shear Slowness
Company:	• Origin Energy Resources Ltd
Well(s):	• Trefoil-1
Interval:	• 2420 to 650m MD (1770m)
Analysis Date:	• September 6th, 2005
Logging Date:	• Nov 24th, 2004
Location:	• Schlumberger Data Services Centre • Perth, Western Australia
Analyst(s):	• Sylvia Tokic
Logging Engineer:	• Josie Robertson

Prepared by:
Sylvia Tokic
Schlumberger Oilfield Australia Pty Ltd
Data & Consulting Services
Level 5, 256 St Georges Terrace
Perth WA 6000
Telephone: +61-8-9420-4800/812
Facsimile: +61-8-9322-3080
mailto:dcs@perth.oilfield.slb.com
stokic@perth.oilfield.slb.com

*Mark of Schlumberger

1 Executive Summary

The DSI* (Dipole Shear Sonic Imager tool with Upper Dipole (UDP), Lower Dipole (LDP) and Monopole (MPS) mode) logs were acquired in vertical exploration well Trefoil-1 (Longitude 145°22'30.87" East and Latitude 39°51' 41.58" South) logged on the 24th of November 2004. Open hole data was processed on the 17th of January, 2005 and cased hole data was processed on the 6th September, 2005 after a request from Origin Energy Resources Ltd. This report discusses the cased hole results.

The data was acquired in both 8.5in open hole section and 9.25in cased hole section, with water-based mud (Seawater/Drispac/Soltex). Measurements were made both in MPS and Dipole modes from TD to 1697m MD and a further MPS downlog was acquired from 280 to 2390m MD. Subsequently, the entire cased hole interval was processed and analysed to obtain compressional and shear slowness within the cased hole section.

Overall, cased hole data was of mostly good coherency which enabled extraction of a non-continuous compressional slowness from the MPS downlog from 2402 to 650m MD. A non-continuous shear slowness was extracted from the UDP uplog from 2401 to 1692m MD.

TABLE OF CONTENTS

TABLE OF FIGURES

APPENDICES

2 Processing Result and Evaluation

2.1 Cased Hole Upper Dipole (UDP) and Monopole P & S (MPS) Results

Compressional slowness was obtained from the MPS mode processing using both the *Receiver* and *Transmitter Arrays* and used to produce Depth Derived Borehole Compensated (DDBHC) final output. Processing used the latest BestDT-3* technique that is based on STC (Slowness Time Coherence) computation, on GeoQuest's GeoFrame 4.0.3 platform. The final DT compressional (DTCO) is therefore an average of DT output from receiver and transmitter array processing, and used in the computation of the Poisson's ratio and VpVs ratio on the final DSI presentation. **Figure 1** shows a section of the results for cased hole. Using the DDBHC method corrects for any slight eccentralising and unfavourable borehole conditions, such as tool tilt and changes in borehole size.

Figure 2 shows the STC versus depth for the MPS. Note the strong and consistent coherence.

Shear curves were obtained from UDP Processing. Unlike MPS, dipole shear is usually derived using receiver array only. BestDT-3* processing uses sophisticated dispersion correction to give a more accurate true formation shear slowness. This is based on using the entire waveform as opposed to part of a waveform and look up chart, which is used in the field. Refer to **Appendix C** for theory and **Appendix A** for mnemonics description.
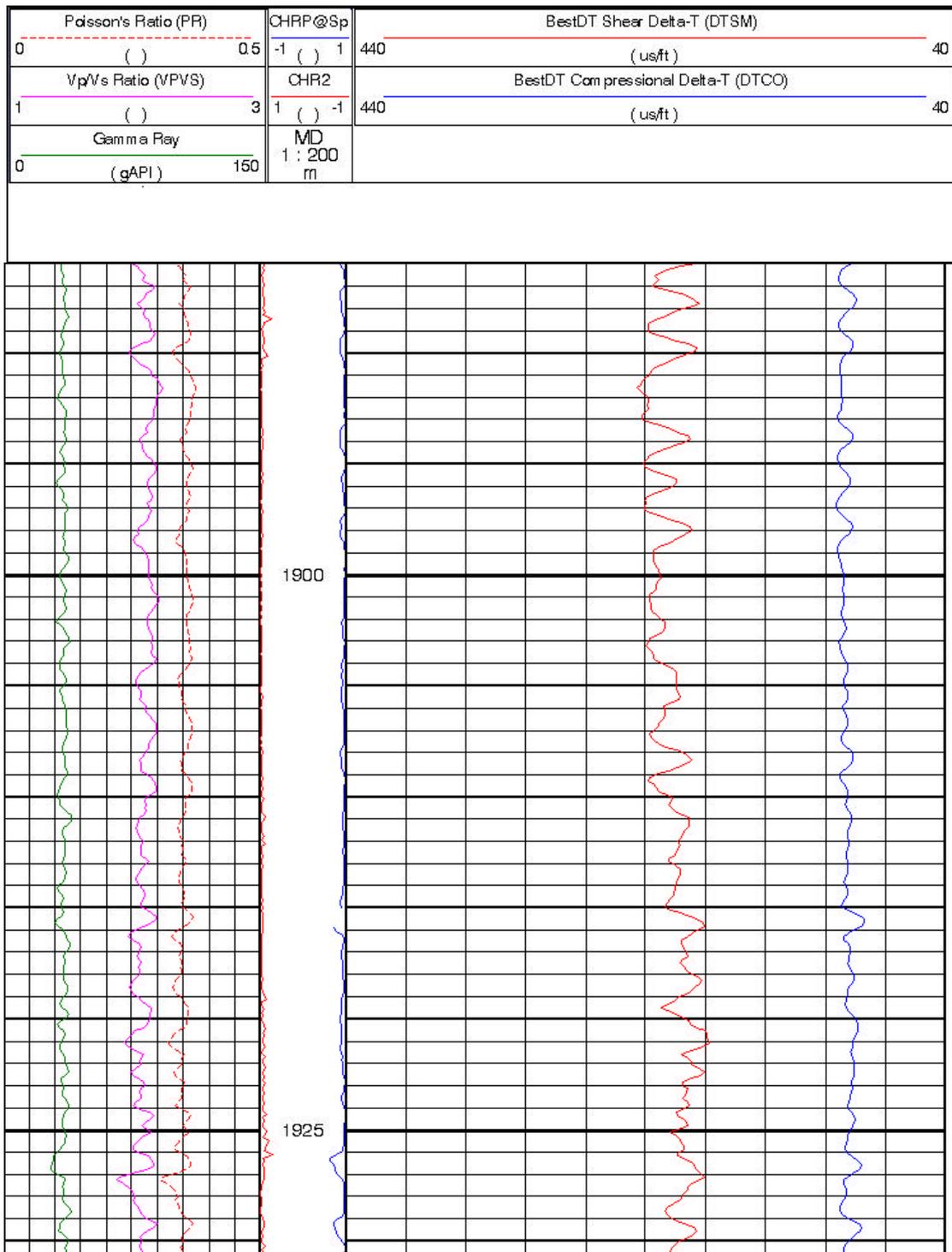
Figure 1: Cased Hole Best DT-3* Results for part of the log

Track 1 shows GR, Poisson's Ratio and VpVS Ratio. See attached print for entire depth section. Depth track contains Label Peak Coherence curves for MPS (blue) and UDP (red), which tend to increase (high uncertainty) across low coherency zones. The last track displays the BestDT-3* results.
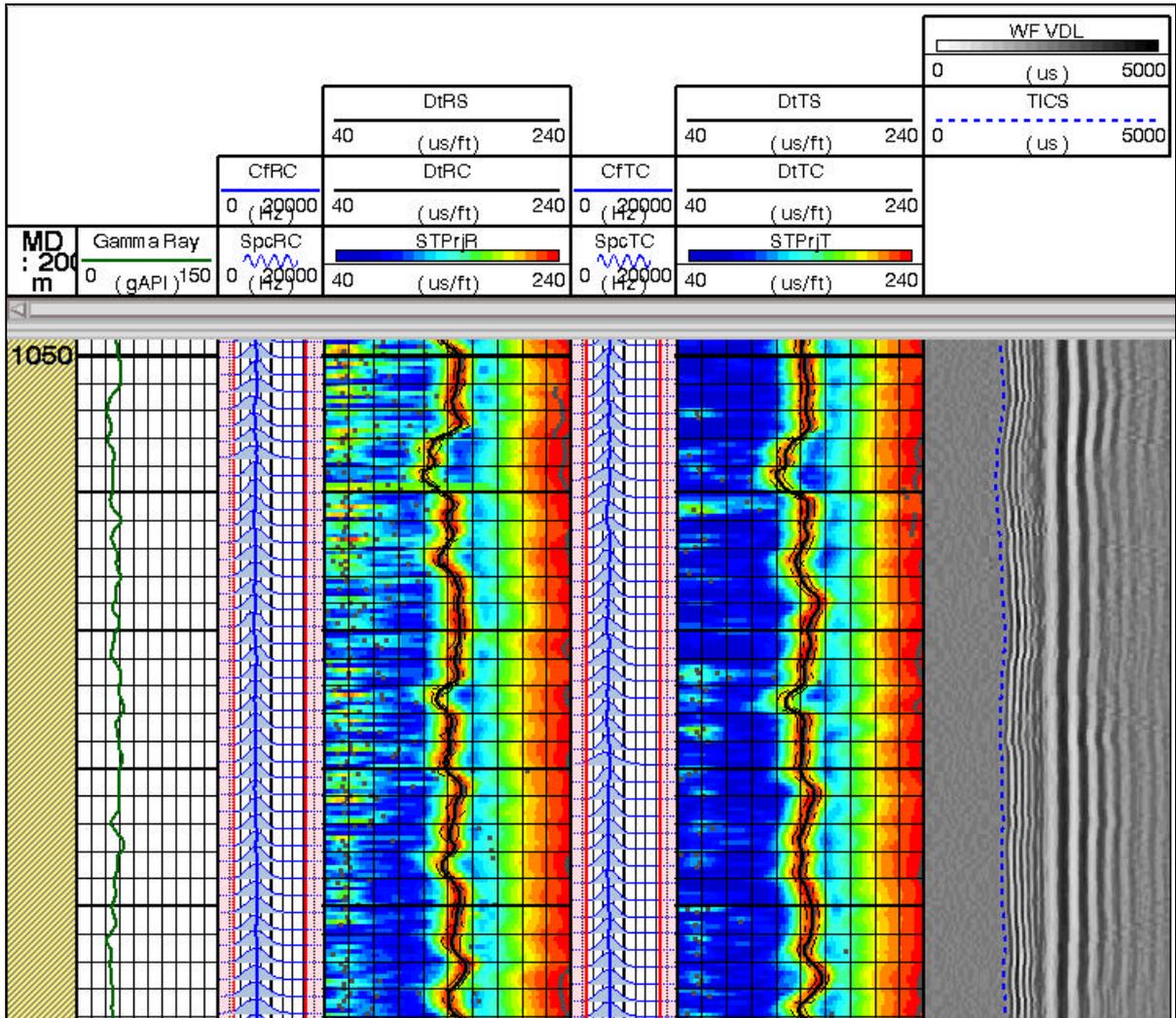
Figure 2: Cased Hole MPS Quality Control for part log

Figure 2, representing the STC quality for cased hole**,** shows that overall, output quality is good, compressional arrivals were shown by strong coherency on both receiver and transmitter array.

Track 1 shows the GR, tracks 2 and 4 show the compressional curve and the frequency window, which the data was processed. Tracks 3 and 5 shows the STC plane in relation to depth. In this example the slowness is very coherent, represented here by a red band. Where the band is not red, the coherency is not as good. This occurs mostly in the shallower sections of the log. The software then selects the most coherent path by using a similar method to 'Tracking and Classification' as discussed in **Appendix C**. Track 6 represents the waveform in variable density log format (VDL). The TICS curve is the compressional transit time. Note that the compressional transit curve matches very well with the first formation arrivals, indicating good quality data whereby the STC semblance processing has detected the correct slowness.

Appendix A: Mnemonics

CfRC	Coherency (Stacked Signal Center Frequency – Receiver Array)
CfTC	Coherency (Stacked Signal Center Frequency – Transmitter Array)
CHRP	Label peak coherence, receiver array – monopole.
CHR2	Label peak coherence, receiver array – upper dipole
CHTP	Label peak coherence, transmitter array – monopole
DDBHC	Depth derived borehole compensated
DT1	Delta-T Shear – Lower Dipole
DT2	Delta-T Shear – Upper Dipole
DT4P	Delta-T Compressional – Monopole P&S
DtRC	Delta-T Compressional – Receiver Array
DtRS	Delta-T Shear – Receiver Array
DtTC	Delta-T Compressional – Transmitter Array
DtTS	Delta-T Shear – Transmitter Array
DTCO	Final BestDT-3* Delta-T Compressional Curve
DTSM	Final BestDT-3* Delta-T Shear Curve
LDP	Lower Dipole Mode
MPS	Monopole P&S Mode
PR	Poisson's Ratio
REC	Receiver
SPcRC	Frequency Spectrum – Receiver Array
SPcTC	Frequency Spectrum – Transmitter Array
STPrjR	STC Slowness Projection – Receiver Array
STPrjT	STC Slowness Projection – Transmitter Array
TICS	Compressional Integrated Transit Time
TISS	Shear Integrated Transit Time
TENS	Tension
UDP	Upper Dipole Mode
VPVS	Ratio of Compressional Velocity to Shear Velocity

Appendix B: Parameters

Table 1: Cased Hole MPS

Parameter	Value	Description
Dtmud	194 us/ft	Mud Slowness
SFTY	Intermediate	Formation Type
HD	8.5 in	Hole diameter
CSIZ	9.625 in	Casing Size
BHS	Cased	Borehole Status
TWI	504 ms	Integrated Time Window
SLL	40	Slowness Lower Limit
SUL	240	Slowness Upper Limit
SST	2	Slowness Step
TLL	504	Time Lower Limit
TUL	4368	Time Upper Limit
TST	168	Time Step
SBW	2730	Search Band Width
SBO	520	Search Band Offset
SWD	20	Slowness Width
TWD	2046	Time Width
SEM	0.35	Semblance Threshold
FLENG	49	Filter Length
FLOW	3000	Filter Band Low
FHIGH	10486	Filter Band High

Table 2: Cased Hole Dipole

Parameter	Value	Description
Dtmud	194 us/ft	Mud Slowness
SFTY	Intermediate	Formation Type
HD	8.5 in	Hole diameter
CSIZ	9.625 in	Casing Size
BHS	Cased	Borehole Status
TWI	1500 ms	Integration Time Window
SLL	80	Slowness Lower Limit
SUL	540	Slowness Upper Limit
SST	4	Slowness Step
TLL	1200	Time Lower Limit
TUL	12800	Time Upper Limit
TST	400	Time Step
SBW	8000	Search Band Width
SBO	1480	Search Band Offset
SWD	60	Slowness Width
TWD	6000	Time Width
SEM	0.35	Semblance Threshold
FLENG	47	Filter Length
FLOW	1000	Filter Band Low
FHIGH	3000	Filter Band High

Appendix C: Theory

Monopole P and S Mode (MPS)

A set of eight monopole sonic waveforms is shown in **Figure 4**. As expected the arrival time of the various arrivals in the waveforms increases with the transmitter-receiver spacing. The slope of a line drawn through the arrival of the same component at each waveform is called the move-out. It represents how much the arrival time is moving out as the distance from the transmitter increases. The moveout can be expressed in µsec/ft and actually represents the slowness of the wave component over the interval covered by the array.
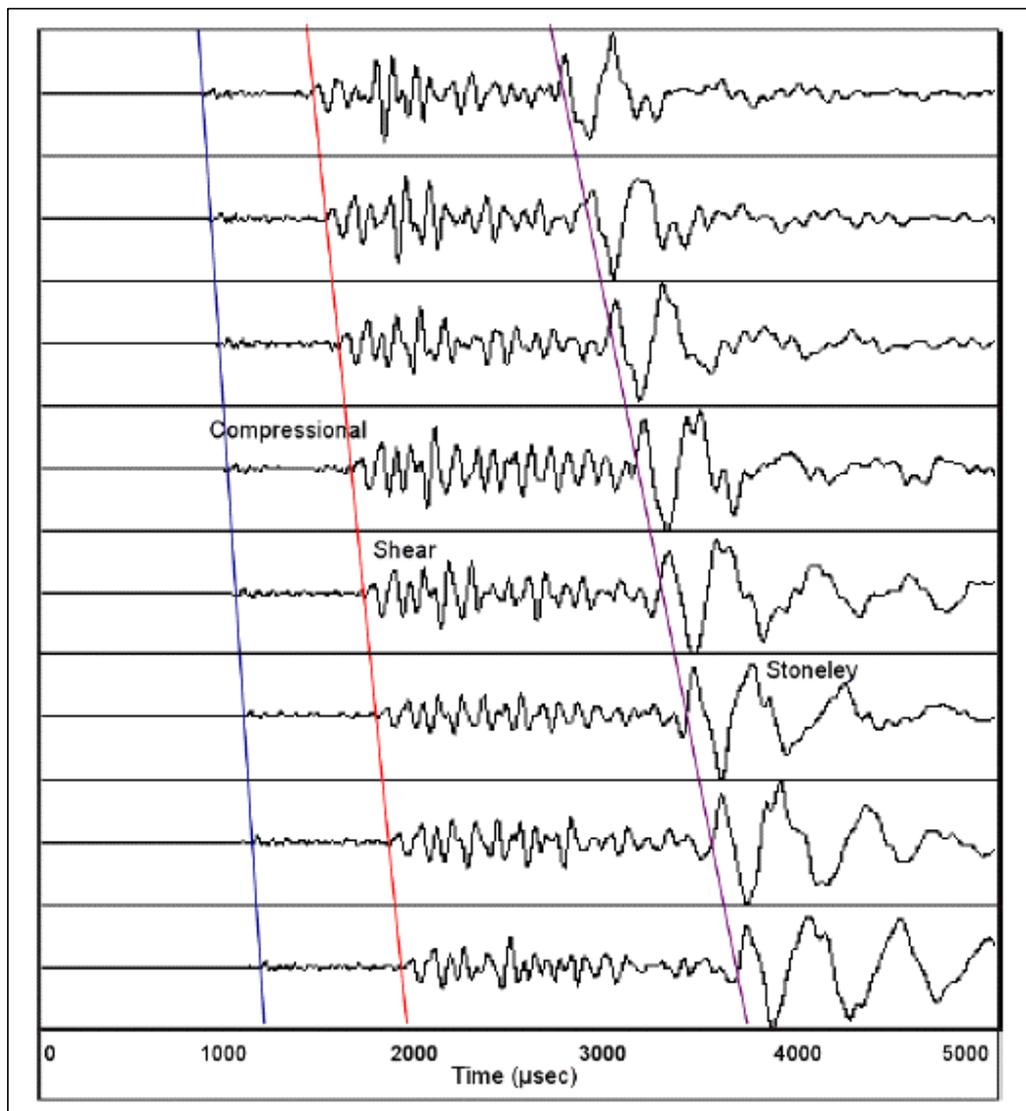

Figure 3: Move-out determination on a set of monopole array waveforms

Slowness time coherence processing, STC, is a processing technique based on semblance that performs this operation automatically. It searches for coherent components along all moveouts in a waveform array. We start by positioning a time window on the reference waveform at time T and then defining a corridor through the array with a move-out S (**Figure 5**). The total or incoherent energy, Ei, is calculated as the sum of the squares of the samples within the corridor (**Eq. 2-1**). The coherent energy, Ec, is then calculated as the arithmetic sum of the samples along the moveout squared (**Eq. 2-2**). When the signal on all waveforms within the window are perfectly correlated, the coherent energy is equal to the total energy times the number of waveforms.

$$E_i(T,S) = \sum_{i=1}^{n} \int_0^{Tw} \left[x_i \left(t - \left[T + S(z_i - z_1) \right] \right) \right]^2 dt \qquad (2\text{-}1)$$

$$E_c(T,S) = \int_0^{Tw} \left[\sum_{i=1}^{n} x_i \left(t - \left[T + S(z_i - z_1) \right] \right) \right]^2 dt \qquad (2\text{-}2)$$

Where i is the waveform number, xi is the value of the waveform sample at time t, Tw the length of the integration time window and zi the waveform depth.
The coherence is defined as:

$$Coh(T,S) = \frac{1}{n} \frac{E_c(T,S)}{E_i(T,S)} \qquad (2\text{-}3)$$

The coherence varies between 0 and 1. A value of 0 means that there is no correlated arrival in the window. On the opposite, a value of 1 means that the waveform components in the window correlate perfectly.
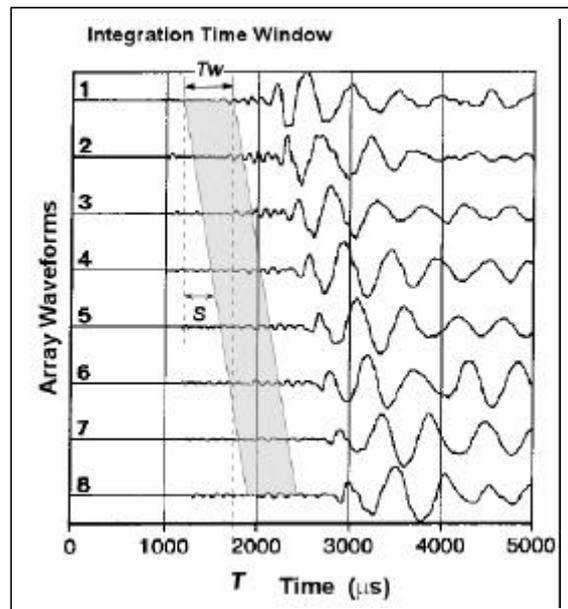

Figure 4: Slowness time coherence computation principle

The computation is done for a range of moveout S, for every possible position of the window in time T. A convenient representation of the coherence results is to display

them on a contour plot versus time and slowness, the ST-Plane (**Figure. 6**). On such a plot each point represents the value of the coherence for a specific time and move out (slowness).

Coherence has a low value unless the integration corridor is positioned over a wave propagating at the considered moveout. Therefore, most of the ST plane is filled with coherence values close to 0 (blue). However, when a coherent arrival is present in the waveforms it shows as a peak of coherence with values that can go up to 1. The process locates the position of the maximum coherence at each peak and outputs the value of slowness, time and coherence in a list. For a given tool configuration, we expect that the time of arrival of a wave will be approximately the product of the slowness by the spacing between the transmitter and the reference receiver. This relation is represented on the plot by the TR line. The ST-plane shown on the example is from a set of monopole waveforms. The three main peaks observed, starting from bottom left, probably represent the compressional, the shear and the Stoneley arrivals. However, at this stage the peaks only represent coherent arrivals in the waveforms and are not identified. The process is repeated for each set of waveforms acquired by the tool at each depth sample.
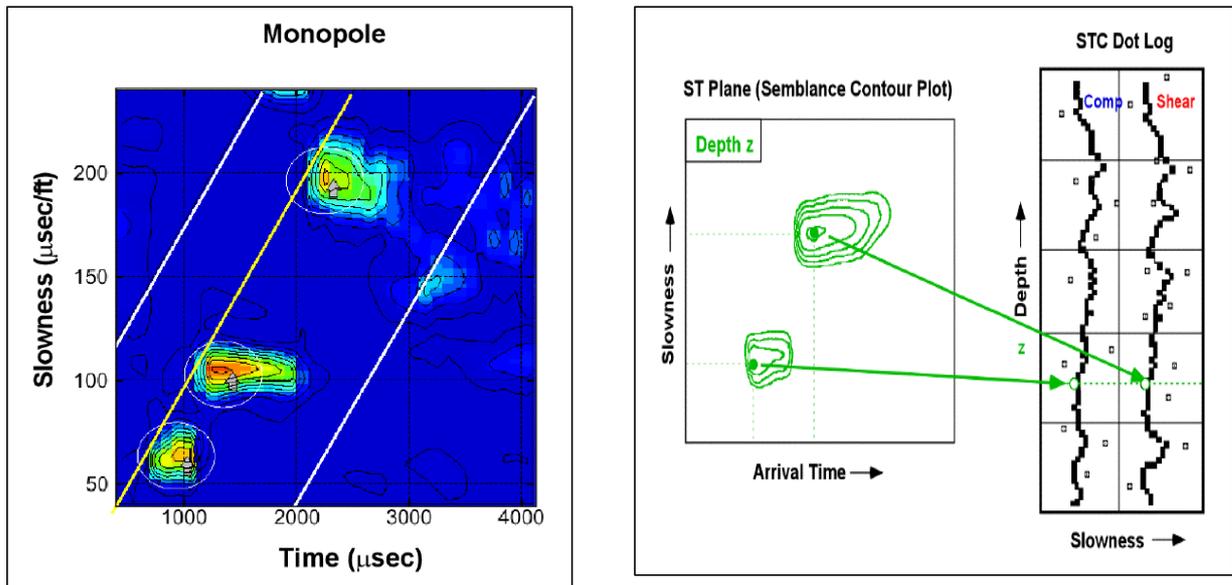

Figure 5: Slowness-Time Plane monopole example. Figure 6: Coherence peak labelling and slowness dot-logs generation

STC processing outputs a list of coherence peaks at every measurement depth. We can represent these peaks as dots on a slowness versus depth plot (**Figure 7**). On such a plot, coherent arrivals display as continuous series of dots. There may also be scattered coherence peaks caused by noise, bed boundaries or other spurious effects that do not match with continuous trends. 'Tracking and classification' identifies the peaks that belong to consistent arrivals versus depth, assigns them to a specific wave type, for example compressional or shear, and output the values in the form of a continuous slowness log. Tracking and classification uses rules to identify the different waves. Typical rules used by tracking and classification are that the peaks have sufficient continuity in depth, sufficient coherence, that the compressional is faster than

the shear arrival and that the ratio of their respective slownesses is larger than 1.45.

Sometimes, dots are missing and there are gaps in the trends. These may originate among other causes from unfavourable borehole conditions, layering or noise. As long as the gap is small, tracking and classification interpolates in between existing peaks to obtain a continuous log, but if the gap is larger than a couple of feet, the log is set to absent.

Upper and Lower Dipole Mode (UDP & LDP)

A flexural wave is propagated through the borehole by inducing a pressure wave perpendicular to the borehole wall and propagates throughout the borehole wall. The borehole wall then experiences a transverse displacement as indicated in **Figure 8,** which is similar to the shear velocity of the formation.
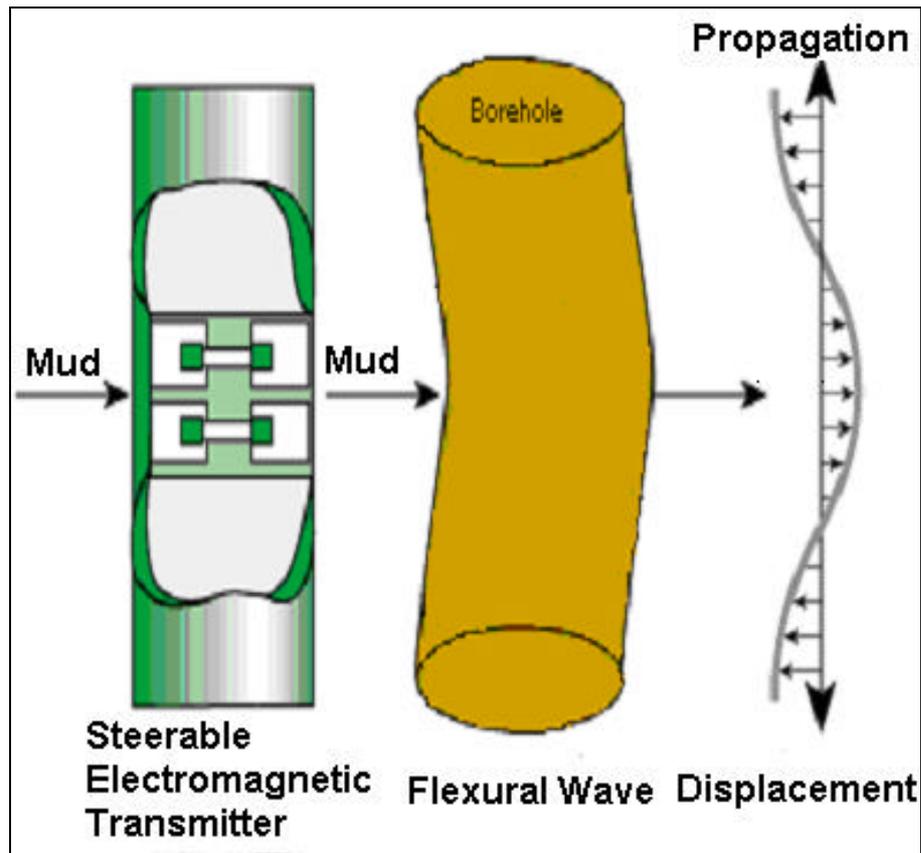

Figure 7: Flexural wave propagation to measure shear velocity

A problem of dispersion effects occurs with shear velocity measurements. Dispersion is the effect of variation of velocity with frequency and makes it difficult to determine a true formation shear. The higher the frequency, the more dispersion occurs. A method known as Bias Correction is applied real time in the field, which basically uses a correction based on numerical modelling. It is also based on a narrow frequency band at low frequencies where dispersion effect is less and so does not take into account the entire waveform. Although this is a fast and simple technique, it is not the best. Best-DT 3* uses a more advanced technique known as Dispersive STC Processing and is based on the entire waveform and uses model dispersion curves to correct for dispersion rather than a look up table, as with Bias correction. Correction is therefore more refined and accurate.

Dispersion depends on frequency, borehole size, formation shear slowness, mud slowness and formation to mud density ratio. In hard formations, mud slowness has less of an effect on dispersion.

Shear Anisotropy Measurement

For sonic measurements, it is well recognized that sedimentary rocks generally exhibit some degree of anisotropy. Anisotropy may arise from intrinsic structural effects, such as aligned fractures and layering of thin zones, or from unequal stresses within the formation. These effects lead to differences in formation elastic properties, and if they are on a smaller scale than the sonic wavelengths, then sonic wave propagation can be used to detect and quantify the anisotropy.

Sonic waves travel fastest when the direction of particle motion (polarization) is aligned with the material's stiffest direction. Shear-wave particle motion is in a plane perpendicular to the wave propagation direction. If the formation is anisotropic in this plane, meaning that there is one direction that is stiffer than another, then the shear-wave polarization aligned in the stiff direction will travel faster than one aligned in the other, more compliant direction. As a result, the shear wave splits into two components, one polarized along the formation's stiff (or fast) direction, and the other polarized along the formation's compliant (or slow) direction.

For example, in the case of vertically aligned dense micro-cracks or fractures, a shear wave that is polarized parallel to the fracture strike will propagate faster than a shear wave polarized perpendicular to it (**Figure 9**). In general, a shear (or flexural) wave, generated by a dipole source, will split into two orthogonal components polarized along the X- and Y-directions in the formation. As they propagate along the borehole, the fast wave will be polarized along the direction parallel to the fracture strike and a slow wave in the direction perpendicular to it.

With two orthogonal dipole transmitters and multiple receiver pairs aligned in orthogonal directions, the DSI Dipole Shear Sonic Imager tool can measure the components of shear slowness in any direction in a plane perpendicular to the borehole axis (**Figure 10**). The measurement involves recording the waveforms on receivers pointing in directions parallel and normal to each transmitter along the tool x- and y-axes.

Four sets of waveforms are recorded at each depth and receiver level. These measurements are labelled xx, xy, yx and yy. The first direction refers to the transmitter and the second direction to the receiver. The direction and speed of the fast and slow split shear waveforms travelling in the formation can be easily determined by mathematically rotating the measured waveforms through an azimuthal angle so that they line up with the two orthogonal formation X- and Y-directions. This is done by minimizing the cross-receiver energies, xy and yx.

The rotated direction of the fastest shear wave becomes the fast-shear tool azimuth; and the tool orientation, measured by a magnetometer, is used to determine the fast

shear azimuth relative to true north. This rotation, called the Alford method, uses the fact that the anisotropy model expects the amplitude of the cross-receiver measurements to vanish when the measured axes x and y align with the anisotropy axes X and Y.

In addition to the fast and slow shear-wave velocities, determined by a slowness time coherence (STC) processing on the rotated waveforms, three measurements of anisotropy are computed. These are **energy anisotropy, slowness anisotropy** and **time anisotropy.**
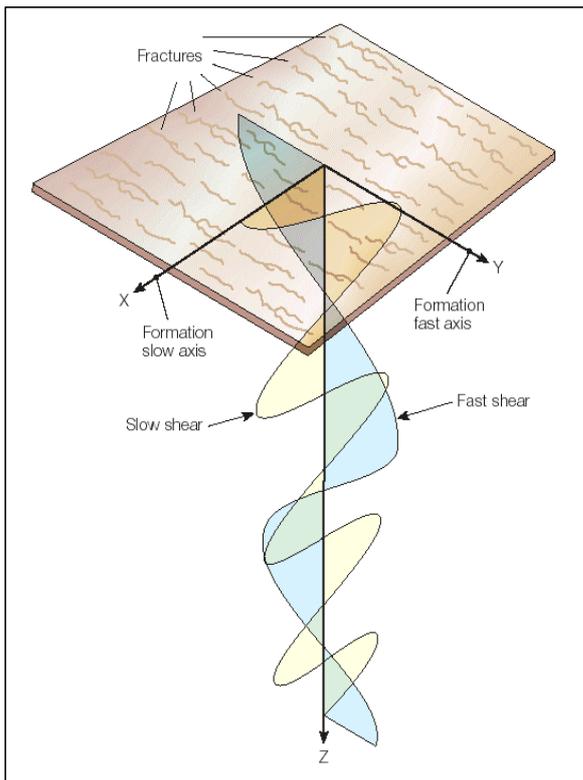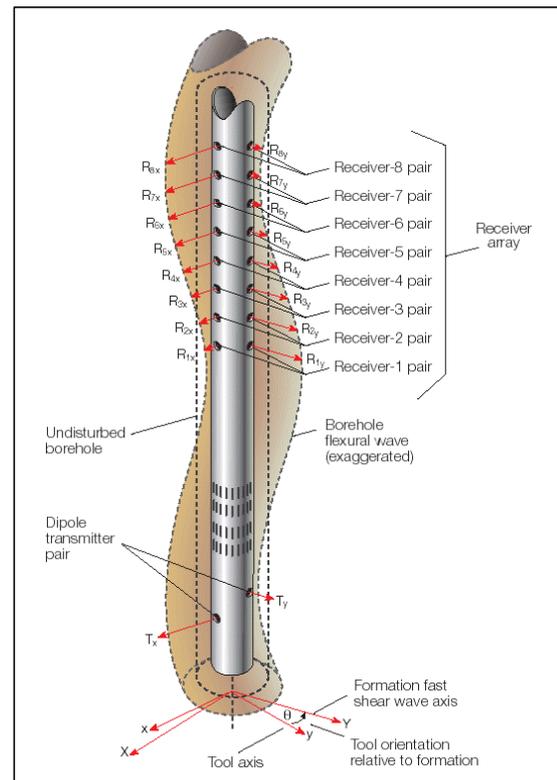

Figure 8: Shear wave splitting Dipole (BCR) Mode

Figure 9: DSI tool showing X-

Figure 9. Shear-wave splitting. Shear waves travel in an anisotropic formation with different speeds along the directions of the formation anisotropy. In this example, anisotropy is caused by the vertical fractures (or micro-cracks) with a strike direction along the formation Y-axis, and the fastest shear wave, with the longer wavelength component, will be polarized along the fracture strike direction as it propagates along the borehole (Z-axis). When shear wave splitting is the result of stress anisotropy, the Y-axis corresponds to the direction of maximum stress, and the X-axis corresponds to the direction of minimum stress.

Figure 10. During logging, flexural waves are induced by dipole transmitters fired sequentially in two perpendicular directions, first along the tool x and then the tool y-

axes. In this example, the fastest component of the induced shear wave is polarized along the formation Y-axis direction, which is aligned along the fracture strike or maximum stress direction. The sloTrefoil-1 component of the shear wave is polarized along the formation X-axis.   Projections of these two shear-wave components are received by each of the dipole sonic tool x- and y-receiver pairs. The inline signals xx and yy are the x-receiver and y-receiver waveforms received when the x and y-transmitters are fired. Cross-signal components xy and yx are the y- and x-receiver waveforms received as the x- and y-transmitters are fired. The Alford rotation angle, q, is determined by minimizing the cross signal components. This would happen automatically if the tool axes were rotated through an angle, q, and aligned with the two orthogonal directions in the anisotropic formation.

Slowness anisotropy is the difference between the fast and slow slownesses calculated by STC on the rotated waveforms. It yields a quantitative measure of slowness anisotropy, and has the best vertical resolution at about 3 ft [1 m]; the size of the receiver array. It can be compared directly with seismic or core measurements of slowness anisotropy.

Travel time anisotropy is the arrival-time difference between the fast- and slow-shear waves at the receivers. It is obtained from a cross-correlation between fast and slow shear-wave arrivals at each receiver spacing. Time lags computed at each receiver are referenced to the largest offset receiver and averaged across the receiver array. This is divided by the average of the fast and slow arrival times to compute a percentage difference. The travel time anisotropy indicator is robust and quantitative, and has the vertical resolution of the average transmitter-receiver spacing, 13 ft [4 m]. Slowness and travel time anisotropy indicators are identical in formations with homogeneous beds thicker than 13 ft.

Energy anisotropy is the energy in the cross component waveforms as a percentage of energy in all four components. In an isotropic formation, energy anisotropy reads zero. In an anisotropic formation, the reading depends on the degree of anisotropy. Two curves are computed from the waveforms: minimum and maximum cross-energy.

The minimum cross-energy is the energy in the cross-components when the tool measurement axis lines up with the formation anisotropy axis. Minimum cross-energy reads zero in an ideal formation whether anisotropic or not. This curve is a good relative measure of whether the assumed model for anisotropy inversion fits the real formation.

The maximum cross-energy is a measure of the amount or strength of anisotropy. Unlike the two previous anisotropy measurements (slowness and time), energy anisotropy is a measure of both slowness and amplitude differences of the fast and slow shear waves. Large differences between the maximum and minimum values, especially when the minimum energy is low, indicate zones of significant anisotropy. Energy anisotropy, though qualitative, is little affected by processing, and is the principal measure of anisotropy.